ISSN NO. 2320-5407

Journal homepage: http://www.journalijar.com

INTERNATIONAL JOURNAL OF ADVANCED RESEARCH

RESEARCH ARTICLE

Electrochemical deposition of nanocrystalline tungsten bronze films on platinum

S.V. Vakarin[1]*, O.L. Semerikova[1], A.V. Kosov[1], A.A. Pankratov[1], S.V. Plaksin[1], I.V. Korzun[1], L.A. Akashev[2], Yu.P. Zaikov[1]

1. Institute of High-Temperature Electrochemistry of UB RAS, st. Akademicheskaya 20, Yekaterinburg, Russian Federation, 620990
2. Institute of Solid State Chemistry of UB RAS, st.Pervomayskaya 91, Yekaterinburg, Russian Federation, 620990

Manuscript Info

Manuscript History:

Received: 15 June 2015
Final Accepted: 22 July 2015
Published Online: August 2015

Key words:

Nanostructures, Electrochemical growth, Growth from melt, Tungsten bronzes

Corresponding Author

S.V. Vakarin

Abstract

Nanocrystalline films of tungsten oxide bronzes with hexagonal and cubic structures have been deposited on platinum substrates by electrolysis of 0.30 K_2WO_4 - 0.25 Li_2WO_4 - 0.45 WO_3 melt by a pulsed potentiostatic technique in the 700-750 ºC temperature range. The thicknesses of the films obtained are shown to consist of one to several monolayers. The effects of temperature, overpotential, deposition time, and substrate structure on the deposit morphology have been studied. The detailed mechanism of the formation of tungsten bronze films with hexagonal structure on rolled (110)-textured Pt foils as substrates has been suggested. It has been also demonstrated that the hexagonal tungsten bronze films exhibit good thermal stability in a wide 20-800 ºC temperature range.

INTRODUCTION

Tungsten oxide bronzes, or simply tungsten bronzes (TB) are a group of complex compounds generally forming in ternary metal oxide systems. Their chemical form can be thus presented as M_xWO_3**,** where M is mostly an alkali or alkaline earth metal, $0<x<1$. These compounds exhibit unique physical properties, such as high corrosion resistance, variable (depending on the composition) electrical conductivity, selectivity toward certain types of cations in aqeous solutions, color change in a broad spectral range, etc. This makes the TB materials very promising for applications in medicine, electrical engineering in the radio frequency range, food and chemical industries. They can be used for producing ion-selective elements in micro-environmental analysis, electro-chromic displays, cold cathodes, catalysts for chemical reactions and numerous other materials and devices.

Presently, the development of novel effective methods for producing nanomaterials, including nanocrystalline films as organized nanosystems, in which the nanosize emerges only in one dimension, is of great interest both scientifically and technologically [1]. Many diverse methods for obtaining thin nanostructured films have been developed so far. For example, WO_3 thin films have been synthesized by using numerous physical and chemical methods. The former include physical vapor deposition (PVD) from the gas phase [2-6], pulsed laser deposition [7], drop dispersion [8], magnetron sputtering [9, 10], reactive radio-frequency pulverizing [11], thermal evaporation [12, 13], Langmuir–Blodgett technology [14], etc. Among the chemical methods, chemical deposition from the gas phase (CVD) [15, 16], electrodeposition [17, 18], and sol-gel deposition [19, 20] are most efficient.

We had studied earlier [21] the growth rate anisotropy and morphology of potassium-lithium tungsten oxide bronze single crystals formed during the electrolysis of a 0.30 K_2WO_4 - 0.25 Li_2WO_4 - 0.45 WO_3 melt at 700° C under potentiostatic conditions with the overpotential ranging from 0 to 70 mV. An anomalous decrease in the growth rate of the $\{10\bar{1}0\}$ faces was observed at the overpotential values exceeding 30 mV. It was suggested that a specific mechanism of selforganization took place in course of the crystal growth process. The selforganization was associated with selection of electroconductivity between separate blocks of the growing crystal.

Recently, we have demonstrated the actual possibility of obtaining nanocrystalline coatings [22] and TB films of nanometric thickness by the electrochemical method. The $K_xLi_yWO_3$ nanofilms of hexagonal TB on a rolled (110)-textured Pt foil have been obtained by electrodeposition from a 0.30 K_2WO_4 - 0.25 Li_2WO_4 - 0.45 WO_3 melt in a pulsed potentiostatic regime at a temperature of 700 °C [23]. The purpose of the present work is to extend these studies in order to elucidate the exact nature of physical mechanisms underlying the electrodeposition of $K_xLi_yWO_3$ TB nanocrystalline films. This investigation encompasses the effect of various processing parameters, such as temperature, overpotential, deposition time, and substrate structure on the deposit morphology as well as on thermal stability of the obtained films.

1. Experimental

1.1 Electrochemical deposition

The kinetics of $K_xLi_yWO_3$ nanofilm electrodeposition was studied using 0.30 K_2WO_4-0.25 Li_2WO_4-0.45 WO_3 melt in ambient atmosphere at 700 and 750 °C. The starting materials were analytically pure K_2WO_4 and Li_2WO_4 and superpure grade WO_3 powders. They were dried at temperatures ranging from 200 to 300 °C for several hours, weighed with the accuracy of ± 0.01 g and mixed in ratios defined above. The mixed powder batch was melted in a platinum crucible, heated above the melting point for a few hours, and transferred into an electrochemical cell. The latter was accommodated in a vertical resistance furnace equipped with the R25.3.2 temperature controller. The operating temperature was sustained with an accuracy of ±1°C. It was measured with Pt-Pt13%Rh thermocouple immersed into the electrolyte close to the electrodes.

Electrolysis was carried out by the pulsed potentiostatic method in a three-electrode cell. A platinum wire served as an anode; a platinum foil with a surface area of 1 cm^2 was employed as a reference electrode which was semi-submersed into the melt. The cathode, a rolled (110)-textured Pt foil, was preliminary cleaned in ethyl alcohol and annealed in air at 700 °C for over 2 hours. A platinum crucible served as a container. The PI-50-1.1 (Russia) potentiostat was used as a power supply. The magnitude and duration of the overpotential pulse were controlled using a PR-8 (Russia) programmer. The detailed schematic drawing of the electrochemical cell and an extended description of the experimental technique are given elsewhere [22, 24]. The cathode was immersed into the melt at the 760 mV equilibrium potential and then overpotential pulse was set.

The potentiostatic current-time transients (*I-t* curves) was registered with the AUTOLAB PGSTAT302N (Metrohm, Netherland) potentiostat-galvanostat. At each fixed value of the overpotential (200, 250, 300 mV) film deposition was carried out at pulse durations of 0.1, 0.3, 0.5, 1, 5, 10, and 15 s. It was established earlier [22] that nanoneedled deposits of TB are formed at the tungsten cathode in the overpotential range of 200-300 mV. The present choice of a similar overpotential range allowed a convenient analysis of the effect of material and substrate structure on the morphology of deposits obtained.

At the final stage of the experiment the Pt substrate with the deposited films, or cathode deposits, were rinsed in an alkali solution (10-15 wt. % KOH) at room temperature. This procedure was performed in a glass-carbon crucible in excess of 12 hours. Finally, the deposit-covered substrates were rinsed with water and ethyl alcohol and dried.

1.2 Characterization

The deposits obtained by electrodeposition were characterized using the SEM, XRD, ellipsometric, and thermogravimetric methods. The effect of electrochemical parameters on the deposits morphology was studied using the JSM-5900 LV (Jeol, Tokyo, Japan) electron microscope. In order to obtain the phase composition of the cathode products, lattice parameters and volume of elementary cell, XRD analysis was performed using a RIGAKU D/MAX-2200VL/PC (Rigaku Corporation, Tokyo, Japan) automatic diffractometer with a monochromatic CuK_α X-ray source emission and the X-ray power of 40 kV, 30 mA.

The thicknesses of films grown on the surfaces of Pt substrates were determined by ellipsometry [25] using the laser photometrical ellipsometer LEF-3M (Russia) employing the standard “absorptive substrate - transparent film” ellipsometry program. With this method, the accuracy of determination of the film thickness depended largely on the substrate preparation details and characterized by accordance of the optical constants (refraction index n=2.08 and absorption factor k=4.49), obtained by us with the reference data [26]. The technique of substrate preparation chosen for this work contributed an error of ± 0.1 nm to the overall film thickness values determined.

The nanocrystalline deposits were found to belong to the hexagonal bronze structure. They were further tested using “NETZSCH” STA 449C Jupiter® (Germany) simultaneous thermal analyzer in order to study the bronzes thermal stability. This device allows performing thermochemical tests, such as differential scanning calorimetry (DSC), in a wide temperature range. The heating rate in the DSC experiments was 10 °C/min. These studies were performed in an ambient atmosphere, and Al_2O_3 crucibles served as sample containers.

2. Results and discussion

Thin nanometer scale films of TB have been grown on (110)-textured Pt foil substrates by electrodeposition from 0.30 K_2WO_4–0.25 Li_2WO_4–0.45 WO_3 melts at 700 °C under variable processing conditions. Four sample micrographs of the resulting films are shown in Fig. 1. The values of the overpotential (η) and electrical pulse duration (τ) employed and the thicknesses of films (δ) obtained are listed in the figure caption. Based on the indicated parameters, the growth rate of the film is as fast as 15 nm/s at a pulse duration of 0.3 s and an overpotential of 250 mV (Fig. 1(*a*)). When a lower overpotential is applied, e.g. 200 mV, the growth rate slows down to the level of about 4 nm/s. This is valid for a rather broad range of pulse duration values, namely between 0.5 and 5 s, which we have used in a series of our complementary experiments (see also Fig. 1 (*b*)). Considering the tungsten bronze crystal lattice parameters (**a** = 7.33±0.01Å and **c** = 7.54±0.01Å), we realize that in the latter case the thickness of the nanocrystaline film is only a few monolayers thick. This result is quite distinct from the deposition of thicker layers of hexagonal nano-needle clusters on (100)-textured tungsten foil substrates under similar conditions: identical molten salt composition, η = 200 mV and τ = 0.5 s [22, 27].

The XRD results show that the overpotential plays a crucial role in determining the film's crystallographic structure. We have been established that TB films with a hexagonal structure, isostructural with the $K_{0.33}WO_3$ compound, form at overpotential lower than 300mV (Fig. 1 (*a*) and (*b*)). The corresponding XRD pattern is shown in the upper part of Fig. 2. On the contrary, bronze films with a cubic structure, isosctructural with the $Li_{0,36}WO_3$ compound, form at overpotential ≥ 300 mV (Fig 1(c, d)). Moreover, at a potential over 300 mV the film breaks down into a "flower-like" morphology which can be clearly observed in the microphotograph of Fig. 1(*d*). In some cases, during a prolonged electrolysis, PtO_2 lines are present in the XRD pattern (Fig. 2). Detailed XRD analysis shows also that platinum oxide is not formed on the Pt substrate in air at temperatures up to 700 °C in course of at least 2 hours. Moreover, platinum oxide has not been ever found on the annealed Pt substrate immersed into the melt during the first 10 minutes without an electrical current flow. Therefore, it may be assumed that platinum oxide forms either directly during electrolysis or right after the current cutoff. It is known [22, 24] that during the TB electrochemical synthesis oxygen ions, O^{2-}, are formed, and they are likely to react with the platinum metal forming an oxide [28, 29].

Apparently, there is an orientational correspondence between cathode surface and the deposited TB film structure and morphology, i.e. the latter is directly related to the substrate structure (texture). A specific example is given in Fig. 1(*b*), where the hexagonal pores within the hexagonal TB film are observed. It is possible to explain the formation of such porous films in the following way. Initially, rounded islets nucleate on the platinum foil, which have preferential azimuthal orientation. This can be explained by the orientational correspondence between the substrate and the deposited material. At a later stage, during the growth process, these islets acquire a hexagonal shape.

Such change in the shape of layers, from rounded to hexagon, was observed at formation of the hexagonal oxide tungsten bronze microcrystal (the technique for crystal growing is described in details elsewhere [24]). The last stage of microcrystal formation is presented in Fig.3. Initially, the layers spreading over the basic plane of the microcrystal are seen to be rounded. After reaching the diameter of 250-300 nm the layers take the form of a hexagon, the boundaries of which are parallel to the forming crystal faces.

Subsequent coalescence of separate islets TB nanofilms into filled crystalline layers is followed by formation of hexagonal pores.

As the TB islets spread over the substrate surface, the stage of their incoherent coalescence is reached leading to the generation of growth imperfections in the form of various crystal lattice defects. These defects serve as active sites [24], at which the dendritic growth begins. The typical dendrite crystals are shown in the microphotograph of Fig. 4.

In order to study the peculiarities of the initial stages of nanofilm formation the chronoamperometry technique has been employed. Fig. 5 shows the current-time curves (*I-t)* taken under various electrodeposition conditions. The actual parameters are indicated in the figure caption. Clearly, in all cases, a sharp rise of the cathode current occurs at the moment of the electrical pulse application. This is quite likely associated with the simultaneous formation of the TB islets on the platinum surface and the beginning of their spreading out process. Such assumption is in god agreement with the theory of collective growth of TB crystals in accordance with the principle of geometrical selection firmly based on the principle of the simultaneous crystal formation at the electrode [24].

Further time evolution of the *I-t* curves shows that the cathode current typically decreases and reaches a minimum value, which is due to coalescence of the TB islets. The subsequent rise of the cathode current which is also observed under all processing parameters can be explained by an increase of the electroactive surfaces due to the formation and growth of the separate crystals on the active sites. We recall that this occurs at the stage incoherent coalescence of the TB islets. It is also apparent from Fig. 5 (curves 1-3) that higher overpotential yield higher cathode currents. This results in a faster coalescence of the TB islets, and the cathode current minimum is reached earlier.

A comparison of the *I-t* characteristics of curves 3 and 4 in Fig. 5 shows that when the electrodeposition temperature is raised from 700 to 750 °C the current minimum is reached at a later time. This implies that a longer time is required for the coalescence of islets with hexagonal structure. In this case, the deposit morphology changes as well. Fig. 6 demonstrates that dendrites grow along with the basic film. We have reported earlier [22] that an increase of the process temperature leads to a change in the morphology of the TB crystals due to the anisotropy of their growth rate. In fact, flat crystallites turn into prisms when the growth rate in the <0001> direction becomes higher than that in the direction perpendicular to it. We presume that the TB film islets on the platinum substrate behave in a similar way, namely: they grow faster in the direction perpendicular to the substrate rather than along its surface at higher temperatures. As a result, there is a delay in coalescence of the TB islets.

We reiterate that the TB nanocrystalline film growth described above is typical for the case of using (110)-textured flat Pt foils as substrates. In other cases, like when platinum a wire is used as an electrode, hexagonal needles are deposited on its surface [30]. Such a deposit is shown in Fig. 7.

Finally, we address the thermal properties of the potassium-lithium tungsten oxide bronze nanofilms with a hexagonal structure grown on the (110)-textured Pt substrates. The results of the differential scanning calorimetry (DSC) analysis are presented in Fig. 8. Curves 1-4 related to the nanofilms exhibit weak negative heat flow minima (as opposed to the distinct broad minimum representing a TB single crystal) indicate the presence of weak exothermic processes. The reproducibility of the baseline (or the instrument error) has been ± 2.5 mW. Therefore, the observed exothermic effects featuring the films are within instrumental error. Nevertheless, the regularity of the DSC signal altering with the film thickness change is clearly detectable. The thicker is the nanofilm, the more pronounced is the thermal effect, and the shallow maxima are shifting to the higher temperature range. It has been found that diffusion of alkali metal ions from the film volume to its surface takes place with a subsequent oxidation by the atmospheric oxygen. Since the volumes in the thin films are very small, the observed thermal effects are practically negligible. In fact, the thermal effect value in the single crystal is relatively small as well. This fact allows to infer that the TB nanocrystalline films obtained under the growth parameters used in this work maintain a good thermal stability. Our preliminary thermogravimetric (TG) measurements have revealed that the weight loss of the hexagonal nanocrystalline TB samples does not exceed 0.2%, namely does not exceed the experimental error, upon heating up to ca. 800 ºC.

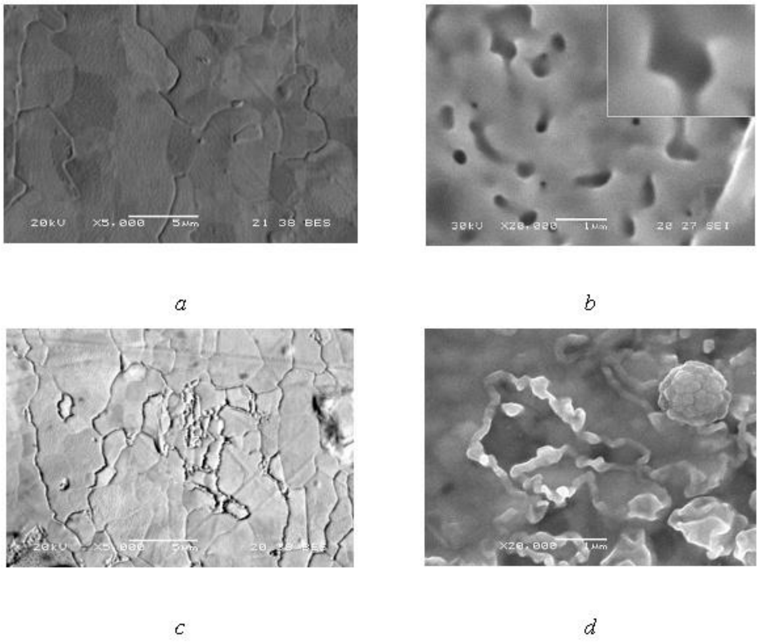

Fig. 1. Microphotographs of TB films grown on (110)-textured Pt foil substrates at T = 700 °C:
***a*) η = 250 mV, τ = 0.3 s, δ = 4.5 nm; *b*) η = 200 mV, τ = 5 s, δ = 20 nm (an enlarged pore image is shown in the upper right corner); *c*) η = 300 mV, τ = 0.1 s, δ = 0.5 nm; d) η = 310 mV, τ = 0.1s.**
***a*) and *b*) represent hexagonal structure films, *c*) and *d*) - cubic structure films.**

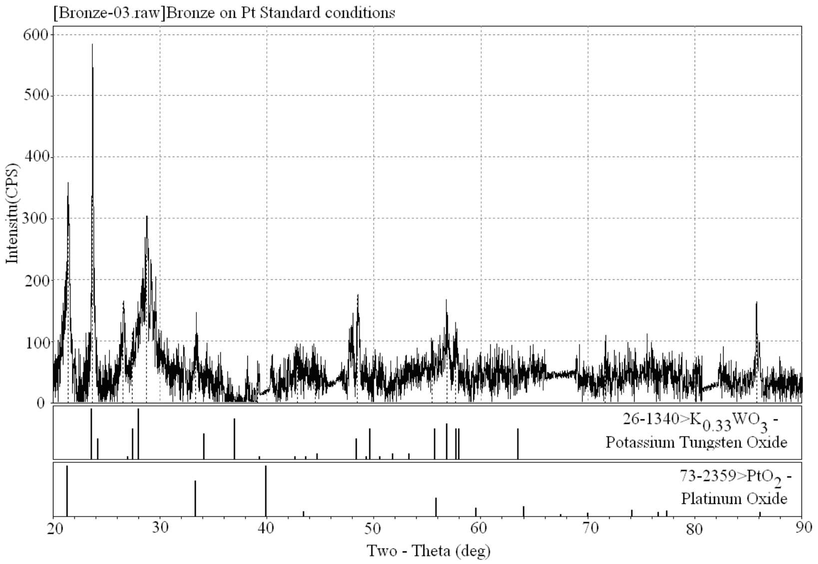

Fig. 2. XRD pattern of the TB film with hexagonal structure deposited on a (110)-textured Pt foil substrate, η = 200 mV, τ = 5 s. The platinum lines are deleted.

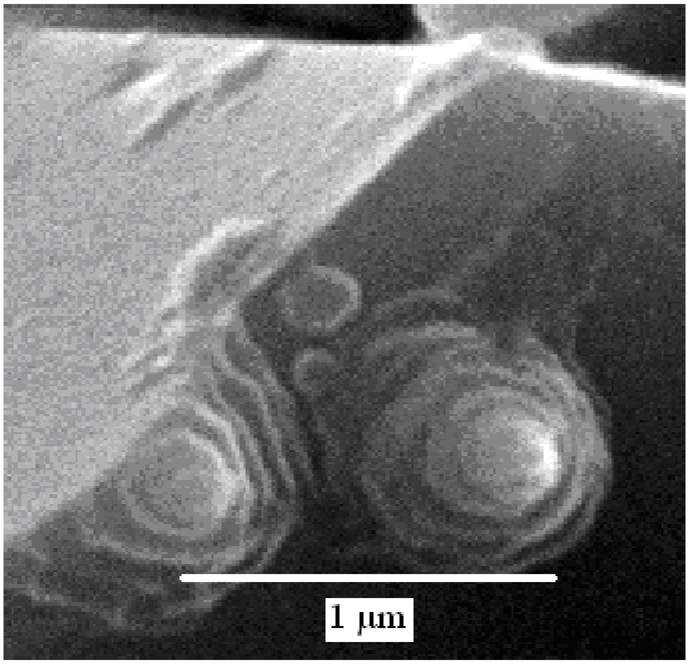

Fig. 3. Last stage of the TB hexagonal submicron size crystal formation. Film layers spread across the (0001) surface.

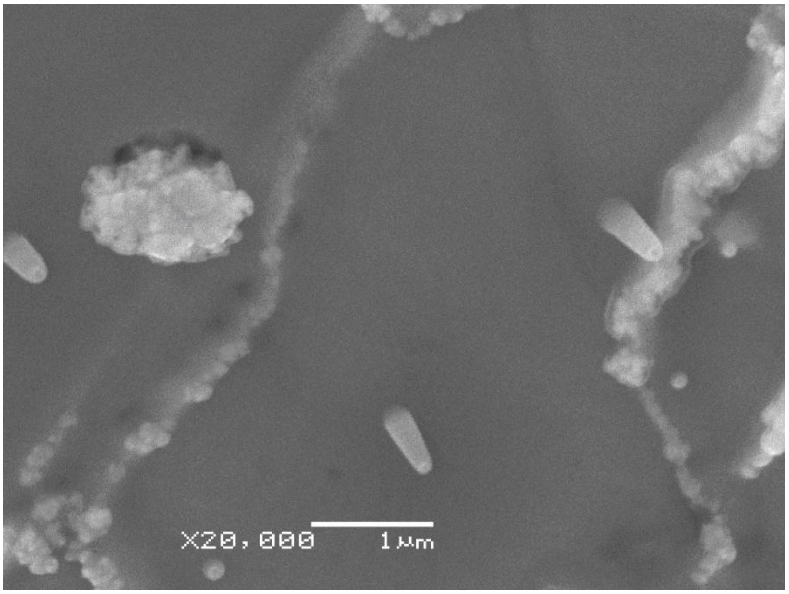

Fig. 4. Appearance of dendritic crystals on active nucleation sites of the TB film grown on a Pt foil substrate. *T* = 700 °C, *η* = 300 mV, *τ* = 1 s.

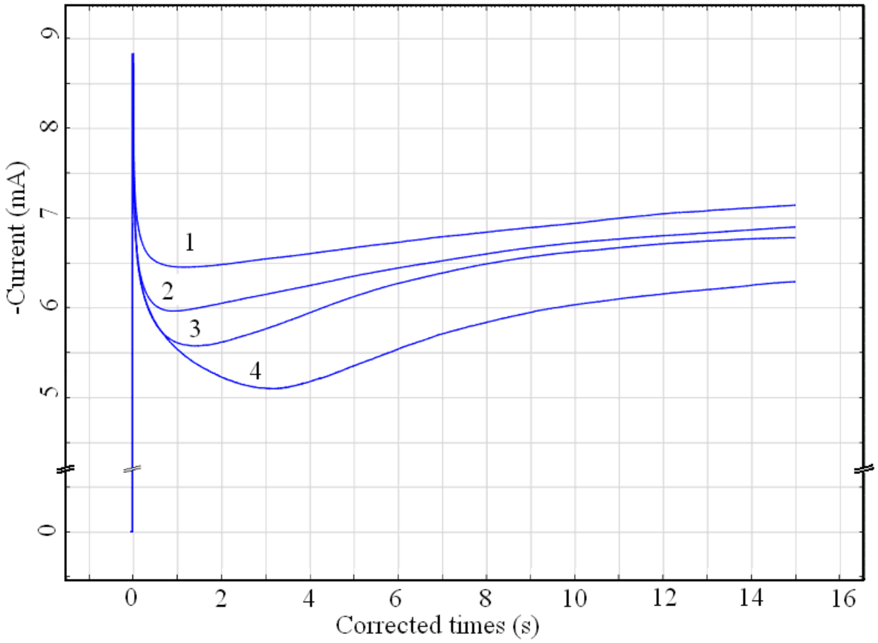

Fig. 5. Current-time curves recorded during the process of TB film deposition on a (110)-textured Pt foil. 1) *η* = 300 mV, 700 °C; 2) *η* = 250 mV, 700 °C; 3) *η* = 200 mV, 700 °C; 4) *η* = 200 mV, 750 °C.

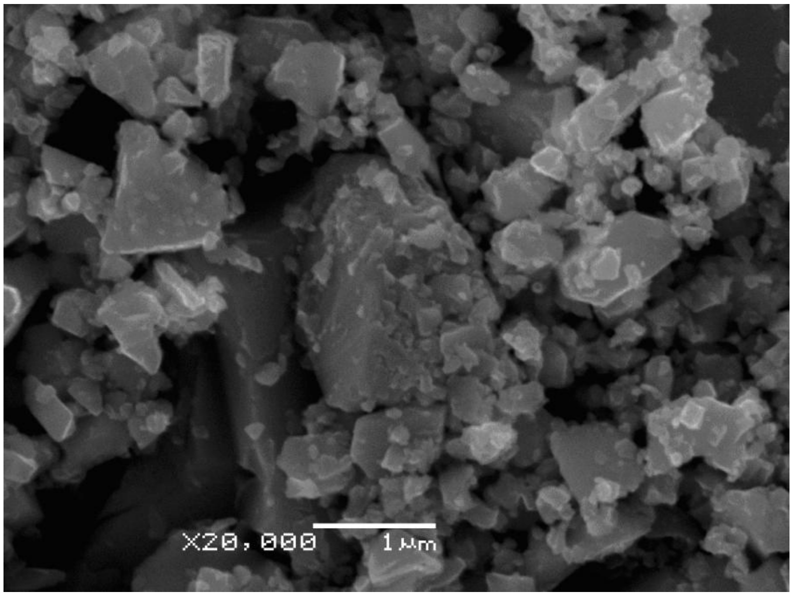

Fig. 6. TB deposit morphology on a (110)-textured Pt foil at *T* =750°C, *η* = 200 mV, *τ* = 5 s.

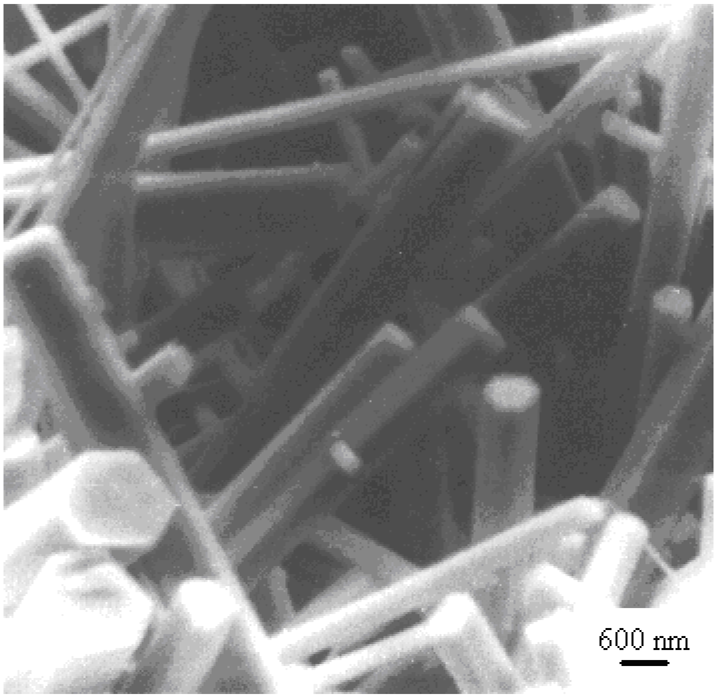

Fig. 7. Section of the TB needled deposit with hexagonal structure grown on a platinum wire electrode.

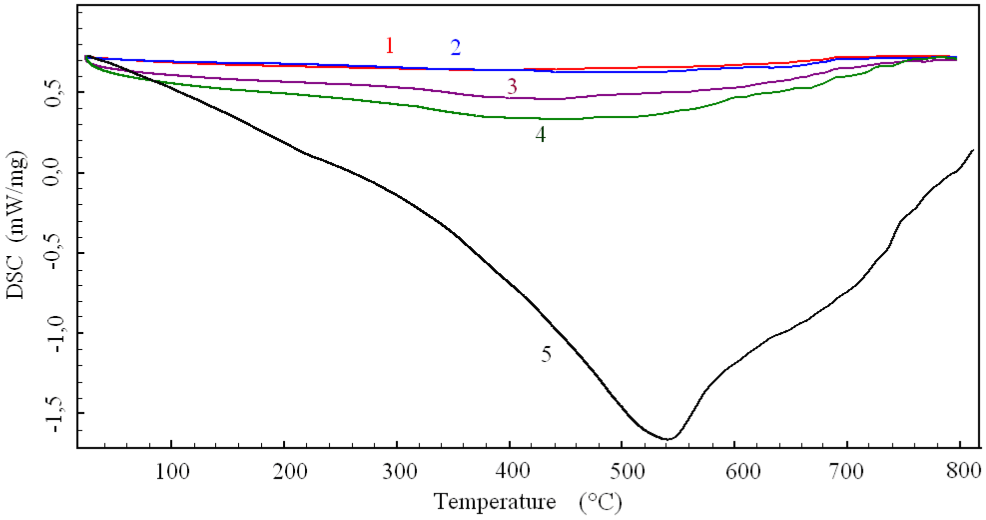

Fig. 8. Temperature dependence of the heat flow (DSC) of TB nanofilms with hexagonal structure deposited on a (110)-textured Pt foil (curves 1-4) and a TB single crystal (curve 5).
1) δ= 0.5 nm; 2) δ= 2 nm; 3) δ=4.5 nm; 4) δ= 20 nm.

Conclusions

We demonstrate for the first time that formation of nanocrystalline TB films with both hexagonal and cubic structures on (110)-textured Pt-foil substrates can be achieved by electrolysis of molten salts. The film thickness is on a nanometer scale and, considering the TB unit cell parameters, it ranges from one to a few monolayers. If the electrolysis is conducted at 700 °C the TB films with a hexagonal structure (isostructural with the $K_{0.33}WO_3$ bronze) forms at overpotentials < 300mV, while the TB film with a cubic structure (isostructural with the $Li_{0.36}WO_3$ bronze) forms at overpotentials ≥ 300mV. At overpotentials > 300mV the smooth film morphology disrupts, and flower-like structures emerge.

At the initial stages of TB films with a hexagonal structure multiple islets are formed on the (110)-textured Pt substrate simultaneously. Their continuous growth is followed by an incoherent coalescence leading to the formation of active sites, at which new crystals, including dendrites, begin to grow. This growth kinetics is associated with the existence of the orientational correspondence between the TB crystal lattice and the substrate structure. It differs from the nanoneedle deposit formation through electrolysis of similar melts on Pt wire or (100)-textured tungsten substrates.

The processing temperature increase from 700 to 750 °C results in formation of dendrites at the cathode (Pt substrate) along with the TB film with hexagonal structure. We assume that the temperature increase causes the TB islets to grow faster in the direction perpendicular to the substrate than along its surface.

The DSC thermal analysis of the TB nanofilms with hexagonal structure has indicated that they exhibit a good thermal stability in the 20 - 800 °C temperature range.

Acknowledgement

The study is supported by Program of UD RAS, project No 15-6-3-21

References

[1] I.P. Suzdalev, Nanotechnology: physico-chemistry of nanoclusters, nanostructures, and nanomaterials (Synergetics: from past to future), Moscow, KomKniga, 2006.
[2] A. Subrahmanyam, A. Karuppasamy, Optical and electrochromic properties of oxygen sputtered tungsten oxide (WO_3) thin films, Sol. Energy Mater. Sol. Cells. 91 (2007) 266-274.
[3] E. Washizu, A. Yamamoto, Y. Abe, M. Kawamura, K. Sasaki, Optical and electrochromic properties of RF reactively sputtered WO_3 films, Solid State Ionics. 165 (2003) 175-180.

[4] M. Stankova, X. Vilanova, E. Llobet, J. Calderer, C. Bittencourt, J.J. Pireaux, X. Correig, Influence of the annealing and operating temperatures on the gas-sensing properties of RF sputtered WO_3 thin-film sensors, Sens. Actuators B: Chem. 105 (2005) 271-277.

[5] A.H. Jayatissa, S.T. Cheng, T. Gupta, Annealing effect on the formation of nanocrystals in thermally evaporated tungsten oxide thin films, Mater. Sci. Eng. B. 109 (2004) 269-275.

[6] I. Porqueras, E. Bertran, Efficiency of Li doping on electrochromic WO_3 thin films, Thin Solid Films. 377-378 (2000) 129-133.

[7] A. Rougier, F. Portemer, A. Qud, M. El Marssi, Characterization of pulsed laser deposited WO3 thin films for electrochromic devices, Applied Surface Science. 153 (1999) 1–9.

[8] S. Pokhrel, C.E. Simion, V.S. Teodorescu, N. Barsan, U. Weimar, Synthesis, Mechanism, and Gas-Sensing Application of Surfactant Tailored Tungsten Oxide Nanostructures, Advanced Functional Materials. 19 (2009) 1767–1774.

[9] M. Bendahan, R. Boulmani, J.L. Seguin, K. Aguir, Characterization of ozone sensors based on WO_3 reactively sputtered films: influence of O_2 concentration in the sputtering gas, and working temperature, Sensors and Actuators B: Chemical. 100 (2004) 320–324.

[10] M. Gillet, K. Aguir, M. Bendahan, P. Mennini, Grain size effect in sputtered tungsten trioxide thin films on the sensitivity to ozone, Thin Solid Films. 484 (2005) 358–363.

[11] C. Bittencourt, R. Landers, E. Llobet, G. Molas, X. Correig, M.A.P. Silva, J.E. Sueiras, J. Calderer, Effects of oxygen partial pressure and annealing temperature on the formation of sputtered tungsten oxide films, Journal of the Electrochemical Society. 149 (2002) H81–H86.

[12] K.J. Patel, C.J. Panchal, M.S. Desai, P.K. Mehta, An investigation of the insertion of the cations H^+, Na^+, K^+ on the electrochromic properties of the thermally evaporated WO_3 thin films grown at different substrate temperatures, Materials Chemistry and Physics. 124 (2010) 884–890.

[13] H. Kim, K. Senthil, K. Yong, Photoelectrochemical and photocatalytic properties of tungsten oxide nanorods grown by thermal evaporation, Materials Chemistry and Physics. 120 (2010) 452–455.

[14] L.M. Blinov, Langmuir films, Physics-Uspekhi (Advances in Physical Sciences). 31 (1988) 623–644.

[15] R.E. Tanner, A. Szekeres, D. Gogova, K. Gesheva, Study of the surface roughness of CVD-tungsten oxide thin films, Appl. Surf. Sci. 218 (2003) 162-168.

[16] T. Ivanova, K.A. Gesheva, G. Popkirov, M. Ganchev, E. Tzvetkova, Electrochromic properties of atmospheric CVD MoO_3 and MoO_3–WO_3 films and their application in electrochromic devices, Mater. Sci. Eng. B. 119 (2005) 232-239.

[17] R. Vijayalakshmi, M. Jayachandran, C. Sanjeeviraja, Structural, electrochromic and FT-IR studies on electrodeposited tungsten trioxide films, Curr. Appl. Phys. 3 (2003) 171-175.

[18] Y.S. Krasnov, G.Y. Kolbasov, Electrochromism and reversible changes in the position of fundamental absorption edge in cathodically deposited amorphous WO_3, Electrochim. Acta. 49 (2004) 2425-2433.

[19] M. Deepa, T.K. Saxena, D.P. Singh, K.N. Sood, S.A. Agnihotry, Spin coated versus dip coated electrochromic tungsten oxide films: structure, morphology, optical and electrochemical properties, Electrochim. Acta. 51 (2006) 1974-1989.

[20] A.Patra, K. Auddy, D. Ganguli, J. Livage, P.K. Biswas, Sol–gel electrochromic WO_3 coatings on glass, Mater. Lett. 58 (2004) 1059-1063.

[21] S.V. Vakarin, A.N. Baraboshkin, K.A. Kaliev, V.G. Zyrianov, Crystal growth of tungsten bronzes with a hexagonal structure, Journal of Crystal Growth, 151 (1995) 121-126.

[22] S.V. Vakarin, O.L. Semerikova, S.A. Surat, A.A. Pankratov, Yu.P. Zaikov. Electrochemical synthesis of nanocrystalline oxide tungsten bronzes with hexagonal structure, Tsvetnye Metally (Non-ferrous Metals). №12 (2013) 45-48.

[23] S.V. Vakarin, A.A. Melyaevaa, A.A. Pankratov, V.A. Kochedykov, L.A. Akashev,
S.V. Plaksin, Yu.P. Zaikov, A method of producing nanocrystalline coatings of oxide tungsten bronzes, Patent RF № 2426822 Published 20.08.2011. Bull.№23.

[24] S.V. Vakarin, Oriented growth of tungsten bronzes at melts electrolysis, Ekaterinburg, Ural Branch of the Russian Academy of Sciences, 2005.

[25] R. Azam, N. Bashara, Ellipsometry and polarized ligh, Moscow, Mir, 1981.

[26] V.M. Zolotarev, V.N. Morozov, E.V. Smirnova, Optical constants of nature and technical media. Handbook, Leningrad, Chemistry, 1984.

[27] S. V. Vakarin, A. A. Melyaeva, O. L. Semerikova, V. S. Kondratyuk, A. A. Pankratov, S. V. Plaksin,
N. M. Porotnikova, Yu. P. Zaikov, L. A. Petrov, Yu. V. Mikushina, A. B. Shishmakov, and O. N. Chupakhin, Catalase activity of coarse-grained and nanosized oxide tungsten bronzes obtained by electrolysis of molten salts, Russian Chemical Bulletin, International Edition. 60 (2011) 1985-1988.

[28] T. Biju Joseph, N Sanil, L. Shakila, K.S. Mohandas, K. Nagarajan, A cyclic voltammetry study of the electrochemical behavior of platinum in oxide-ion rich LiCl melts, Electrochimica Acta. 139 (2014) 394–400.

[29] F. Lantelme, H. Groult, Molten Salts Chemistry: From Lab to Applications, Elsevier Science Publishing, 2013.

[30] S.V. Vakarin, Method for making needle oxide tungsten bronzes, Patent RF № 2354753 Published 10.05.2009. Bull.№13.